

Southwest Pacific vertical structure influences on oceanic carbon storage since the Last Glacial Maximum

Vincent J. Clementi^{1*} & Elisabeth L. Sikes¹

¹Department of Marine and Coastal Sciences, Rutgers University, New Brunswick, New Jersey, USA

Contents of this file

Text S1
Text S2
Figures S1-S5
Tables S1
References

Introduction

We provide information on surface reservoir ages, contouring of vertical isotope differences, five supplemental figures, and a supplemental table of cores used in this study.

Text S1. Radiocarbon surface reservoir ages

In the Tasman Sea cores, ^{14}C -AMS dating on planktic foraminifers was converted to calendar ages using IntCal13 (Marine13), which incorporates a surface reservoir age correction of 400 years [Reimer et al., 2013; Sikes et al., 2016b]. This correction was applied to all ^{14}C dates for the cores. Regional calibration of surface reservoir ages affirms this is valid for the last ~ 17 ka [Sikes and Guilderson, 2016]. For the LGM and early deglaciation, the estimated reservoir age for subtropical waters increases to ~700 years. Incorporation of surface reservoir increases would increase the age estimates by approximately ~300 years for the LGM and early deglaciation for subtropical waters [Sikes and Guilderson, 2016]. This additional correction would not substantially alter the stratigraphy in these cores [Sikes et al., 2016b].

Text S2. Vertical isotope difference contour plot generation

Figure 3 in the main paper plots $\Delta\delta^{18}\text{O}$ and $\Delta\delta^{13}\text{C}$, which have values ranging from -0.2 to -1.8 ‰ and 0.04 to 1.8 ‰, respectively. In Figures 3C and 3D, the contour plots show the differences with depth. For both isotopic records, "blue" is used to indicate relative similarity (0 to 0.67 ‰ for $\Delta\delta^{13}\text{C}$, and -0.67 to 0 ‰ for $\Delta\delta^{18}\text{O}$), while "red" indicates the greater relative differences between SAMW and deeper segments of the water column (1.3 to 2 ‰ for $\Delta\delta^{13}\text{C}$, and -2 to -1.3 ‰ for $\Delta\delta^{18}\text{O}$). "Green" is set at the median range of values and acts as an inflection point between relative similarity and difference from SAMW (0.67 to 1.3 ‰ for $\Delta\delta^{13}\text{C}$, and -1.3 to -0.67 ‰ for $\Delta\delta^{18}\text{O}$). We tested setting the inflection point at values above and below the default median value in additional depth profiles (not shown). This did not remove any trending or observed changes in water column structure, only the saturation of the color spectrum assigned to the vertical gradient calculations. The setting chosen best visualizes similarities above and differences below median value.

Figures S1-S6.

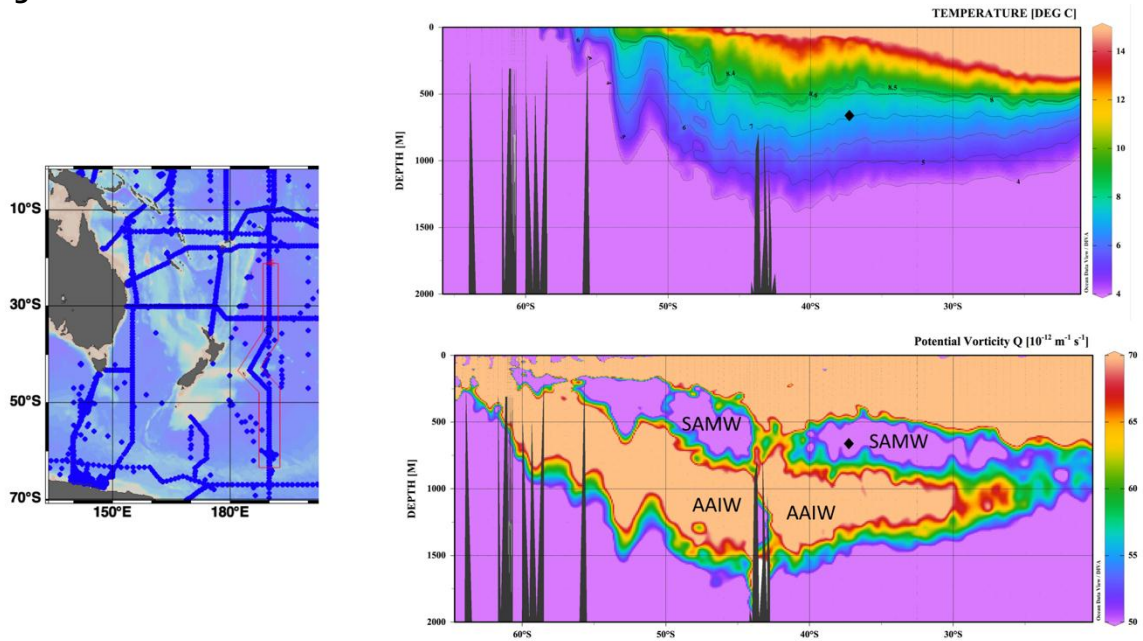


Figure S1a. A meridional transect of the World Ocean Circulation Experiment (WOCE) section P15 for the temperature and potential vorticity parameters. The black diamond represents the depth and latitude of the shallowest core in our depth transect, RR0503-87 (663 m). The major water masses—Subantarctic Mode Water (SAMW) and Antarctic Intermediate Water (AAIW)—are labeled. Core 87JPC sits in SAMW today, which can be defined by a temperature range of 5–8.6 °C and a potential vorticity minimum (e.g., [Chiswell *et al.*, 2015; Hanawa and Talley, 2001; Hasson *et al.*, 2012; Sloyan and Rintoul, 2001]).

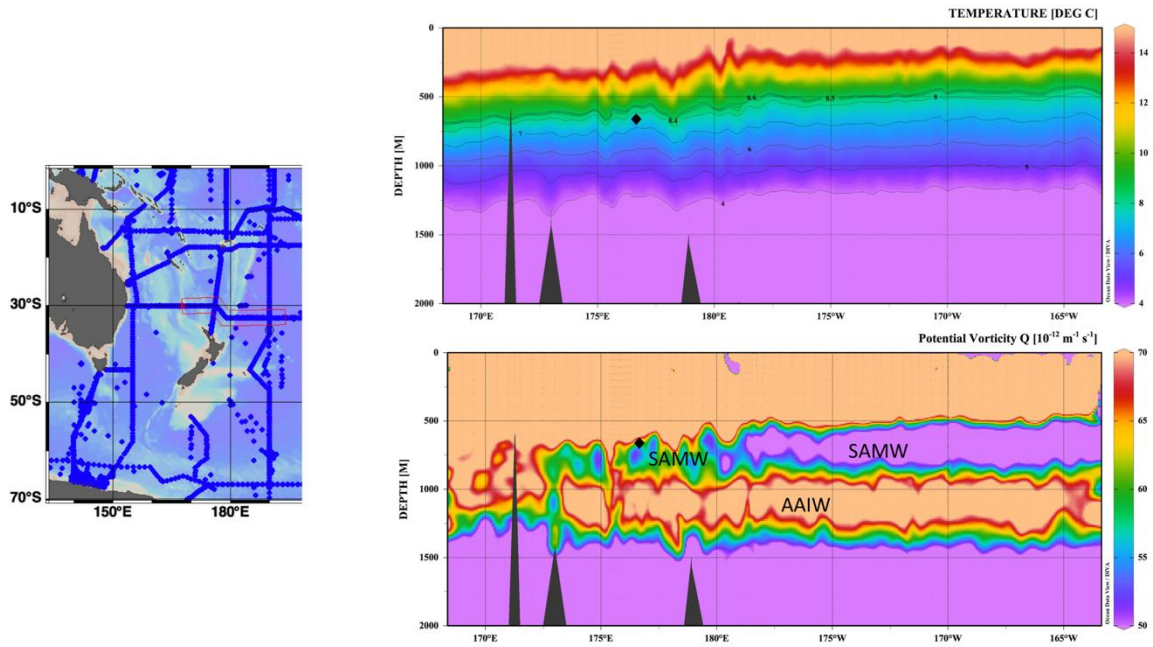


Figure S1b. A zonal transect from the WOCE section Po6, for temperature and potential vorticity. The black diamond represents the depth and longitude of core RR0503-87 (663 m). The major water masses—Subantarctic Mode Water (SAMW) and Antarctic Intermediate Water (AAIW)—are labeled. This confirms the presence of SAMW at the depth of core 87JPC north of New Zealand.

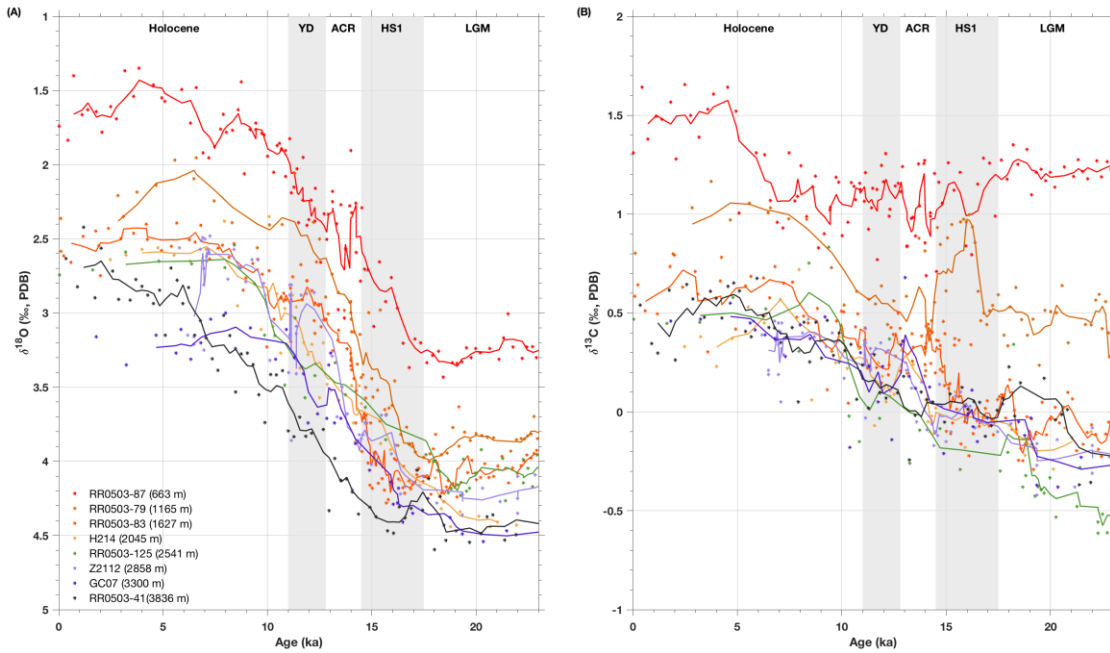


Figure S2. Benthic $\delta^{18}\text{O}$ and $\delta^{13}\text{C}$ data used in this analysis. Compiled $\delta^{18}\text{O}$ and $\delta^{13}\text{C}$ based on *Cibicidoides spp.* These were previously published in [Sikes *et al.*, 2016] and are archived under that publication at <http://www.ncdc.noaa.gov/data-access/paleoclimatology-data>. A) SW Pacific $\delta^{18}\text{O}$. B) SW Pacific $\delta^{13}\text{C}$. Lines are 3-point running means.

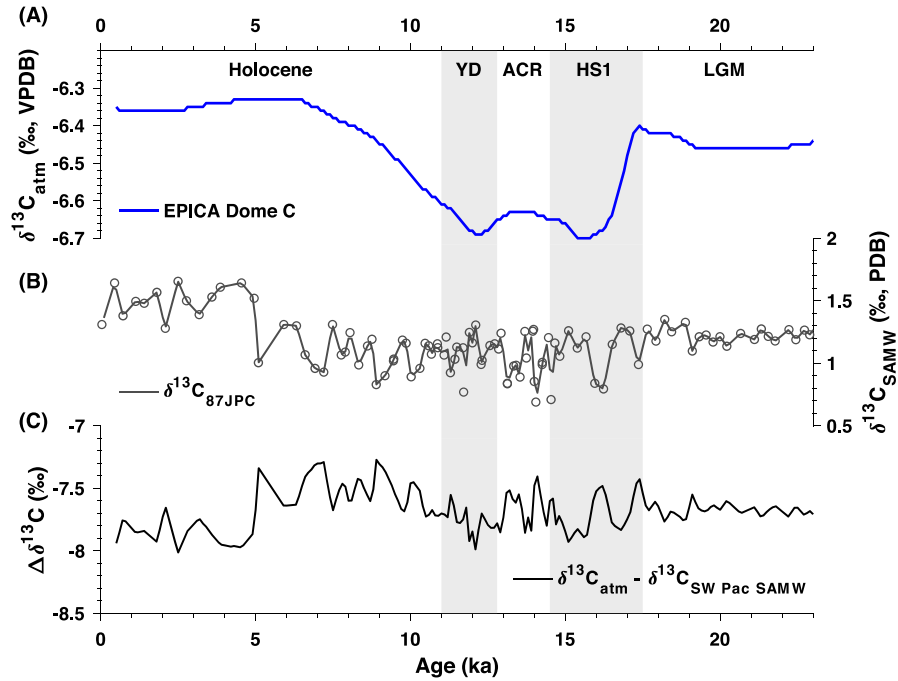


Figure S3. Establishing an atmospheric endmember for vertical isotope difference calculations. Subantarctic Mode Water (SAMW) is a shallow subsurface water mass. The $\delta^{13}\text{C}$ difference between the atmospheric $\delta^{13}\text{C}$ record (A; [Schmitt *et al.*, 2012]) and SAMW for core 87JPC (B) indicates that SAMW $\delta^{13}\text{C}$ in this region was largely in phase with the atmosphere since the LGM (C). The relatively constant offset for the period of this study suggests that the SAMW $\delta^{13}\text{C}$ record in this core is a useful proxy for an atmospheric endmember.

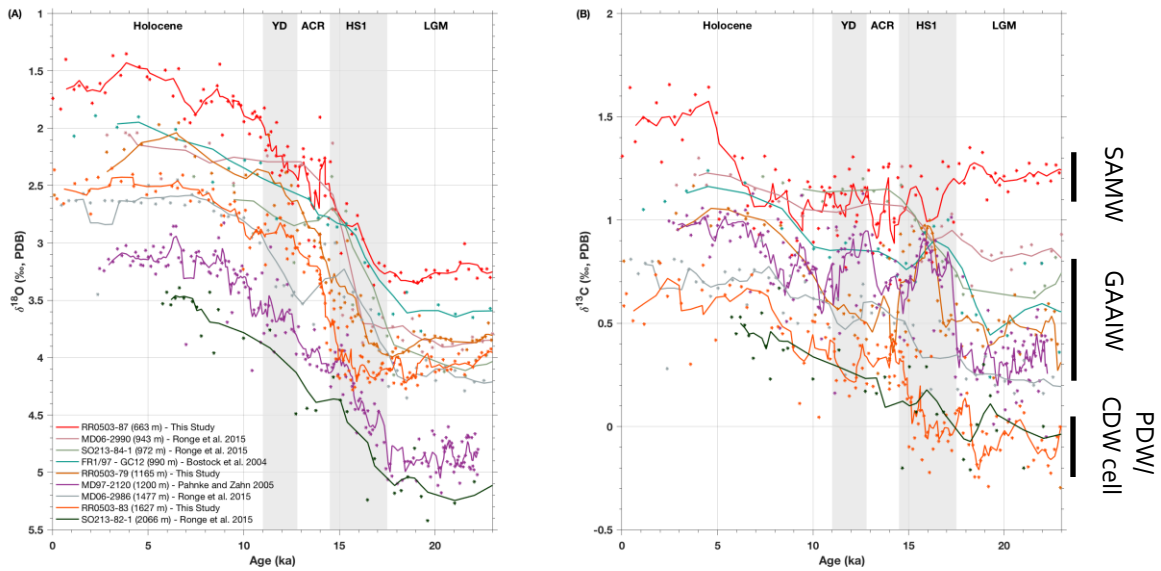


Figure S4. Comparison of regional intermediate water-depth stable isotope records with those used in this study. A) SW Pacific $\delta^{18}\text{O}$. B) SW Pacific $\delta^{13}\text{C}$. Lines are 3-point running means. Vertical black bars in (B) indicate the ranges of glacial water masses. Cores from our depth transect sit at 663, 1165, and 1627 m. We have added here cores MD06-2990 (943 m), SO213-84-1 (972 m), MD06-2986 (1477 m), and SO213-82-1 (2066 m) [Ronge et al., 2015], FR1/97 – GC12 (990 m) [Bostock et al., 2004], and MD97-2120 (1200 m) [Pahnke and Zahn, 2005]. For two of these cores other benthic species were used where Cibicidoides were absent: *Uvigerina peregrina* were used in core SO213-82-1 and *Melonis barleeanum* and *Bulimina aculeata* in core MD97-2120. Interspecies offsets were applied to normalize the infaunal benthic isotopic data (see SOM in [Pahnke and Zahn, 2005] and SOM/Methods in [Ronge et al., 2015]). As a result, $\delta^{18}\text{O}$ in these cores are more positive than others in the compilation making a calculated a $\Delta\delta^{18}\text{O}$ comparison problematic. Regional $\Delta\delta^{13}\text{C}$ are provided in Figure S5. In general, the strong coherence among intermediate-depth $\delta^{18}\text{O}$ suggests a regional signal (A). Regional $\delta^{13}\text{C}$ (B) indicate intermediate and mid-depth waters were both distinct from SAMW, and that mid-depth waters were distinct from intermediate waters, together suggesting the presence of a CO_2 -rich GAAIW and shoaled PDW cell [Pahnke and Zahn, 2005; Ronge et al., 2015]. AAIW-depth $\delta^{13}\text{C}$ became abruptly enriched in concert during HS1, while deeper depths become slowly enriched across the deglaciation.

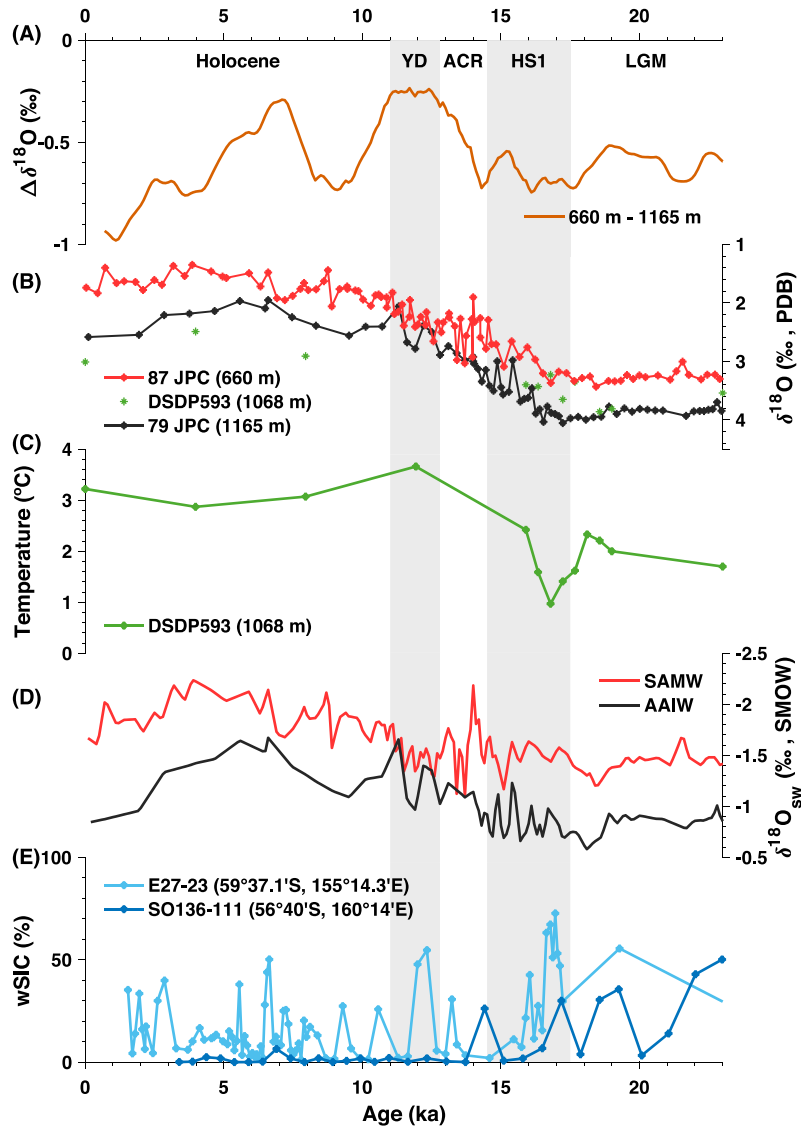


Figure S5. $\delta^{18}\text{O}_{\text{sw}}$ calculation SW Pacific oxygen isotope differences, AAIW temperature, sea ice, and $\delta^{18}\text{O}_{\text{sw}}$ calculation. A) $\Delta\delta^{18}\text{O}$ at 1100 m. B) Regional AAIW-depth $\delta^{18}\text{O}$ (Supplemental Figure 1; [Elmore *et al.*, 2015]). C) Benthic Mg/Ca-derived temperature from an AAIW core in the Tasman Sea [Elmore *et al.*, 2015]. D) Calculated seawater $\delta^{18}\text{O}$ for SAMW and AAIW in the SW Pacific. E) SW Pacific-sector Southern Ocean winter sea-ice concentration since the LGM [Ferry *et al.*, 2015]. Consistent $\Delta\delta^{18}\text{O}$ at 1100 m since the LGM and HS1 (A) suggests these depths were influenced by similar dynamics across this transition, consistent with modern observations [McCartney, 1977]. During HS1, AAIW simultaneously cooled (C) and freshened (D) as Antarctic sea ice approached a minimum (E). Using the Southern Ocean $\delta^{18}\text{O}$ -salinity relationship of $\sim 0.5 \text{ ‰ psu}^{-1}$ [Adkins *et al.*, 2002], we estimate that AAIW at 1100 m freshened by $\sim 1 \text{ psu}$ across the LGM-HS1 transition. We suggest a northward transport of sea ice was integral to this, which prompted the restructuring and rapid ventilation of the upper 2000 m. Table S1. Sediment cores and locations

Core	Depth (m)	Latitude	Longitude	Region	Citation
87 JPC	663	-37.2635 S	176.6643 W	Bay of Plenty	[Sikes et al., 2016]
79 JPC	1165	-36.9587 S	176.5928 W	Bay of Plenty	[Sikes et al., 2016]
83 JPC	1627	-36.7375 S	176.6398 W	Bay of Plenty	[Sikes et al., 2016]
H214	2045	-36.9250 S	177.4417 W	Bay of Plenty	[Samson et al., 2005]
125 JPC	2541	-36.1983 S	176.8892 W	Bay of Plenty	[Sikes et al., 2016]
Z2112	2858	-33.5333 S	166.5333 W	Tasman Sea	[Samson, 1998]
RS147-GC07	3300	-45.1500 S	146.2833 W	Tasman Sea	[Connell and Sikes, 1997]
41 JPC	3836	-39.8773 S	177.6578 E	Hawke Bay	[Sikes et al., 2016]

References

- Adkins, J. F., K. McIntyre, and D. P. Schrag (2002), The Salinity, Temperature, and $\delta^{18}\text{O}$ of the Glacial Deep Ocean, *Science*, *298*, 1769-1773.
- Bostock, H. C., B. N. Opdyke, M. K. Gagan, and L. K. Fifield (2004), Carbon isotope evidence for changes in Antarctic Intermediate Water circulation and ocean ventilation in the southwest Pacific during the last deglaciation, *Paleoceanography*, *19*, 1-15.
- Chiswell, S. M., H. C. Bostock, P. J. H. Sutton, and M. J. Williams (2015), Physical oceanography of the deep seas around New Zealand: A review, *New Zealand Journal of Marine and Freshwater Research*, *49*, 286-317.
- Connell, R. D., and E. L. Sikes (1997), Controls on Late Quaternary sedimentation of the South Tasman Rise, *Australian Journal of Earth Sciences*, *44*, 667-675.
- Elmore, A. C., E. L. McClymont, H. Elderfield, S. Kender, M. R. Cook, M. J. Leng, M. Greaves, and S. Misra (2015), Antarctic Intermediate Water properties since 400 ka recorded in infaunal (*Uvigerina peregrina*) and epifaunal (*Planulina wuellerstorfi*) benthic foraminifera, *Earth and Planetary Science Letters*, *428*, 193-203.
- Ferry, A. J., X. Crosta, P. G. Quilty, D. Fink, W. Howard, and L. K. Armand (2015), First records of winter sea ice concentration in the southwest Pacific sector of the Southern Ocean, *Paleoceanography*, *30*(11), 1525-1539.
- Hanawa, K., and L. D. Talley (2001), Mode waters, in *Ocean Circulation and Climate*, edited by G. Seidler, J. Church and J. Gould, pp. 373-386, International Geophysical Series, Academic Press.
- Hasson, A., A. Koch-Larrouy, R. Morrow, M. Juza, and T. Penduff (2012), The origin and fate of mode water in the southern Pacific Ocean, *Ocean Dyn.*, *62*(3), 335-354.
- McCartney, M. S. (1977), Subantarctic Mode Water, in *A Voyage of Discovery Deep-Sea Research (suppl.)*, edited by M. V. Angel, pp. 103-119, Pergamon, Oxford, U.K. .
- Pahnke, K., and R. Zahn (2005), Southern Hemisphere Water Mass Conversion Linked with North Atlantic Climate Variability, *Science*, *307*, 1741-1746.
- Ronge, T. A., S. Steph, R. Tiedemann, M. Prange, U. Merkel, D. Nürnberg, and G. Kuhn (2015), Pushing the boundaries: Glacial/interglacial variability of intermediate and deep waters in the southwest Pacific over the last 350,000 years, *Paleoceanography*, *30*, 23–38.
- Samson, C. R. (1998), Structure and timing of the last deglaciation in the subtropical and subpolar southwest Pacific: Implications for driving forces of climate, Ph.D thesis, 183 pp, University of Tasmania, Hobart, Tasmania.
- Samson, C. R., E. L. Sikes, and W. R. Howard (2005), Deglacial paleoceanographic history of the Bay of Plenty, New Zealand, *Paleoceanography*, *20*, 1-12.
- Schmitt, J., et al. (2012), Carbon isotope constraints on the deglacial CO_2 rise from ice cores., *Science*, *336*, 711-714.

Sikes, E. L., A. C. Elmore, K. A. Allen, M. S. Cook, and T. P. Guilderson (2016), Glacial water mass structure and rapid $\delta^{18}\text{O}$ and $\delta^{13}\text{C}$ changes during the last glacial termination in the Southwest Pacific, *Earth and Planetary Science Letters*, 456, 87-97.

Sloyan, B. M., and S. R. Rintoul (2001), Circulation, renewal, and modification of Antarctic mode and intermediate water, *J. Phys. Oceanogr.*, 31(4), 1005-1030.